

**Abdulmalik A. Alghamdi**

Associate Professor,  
Department of Mechanical Engineering,  
King Abdulaziz University,  
PO Box 80251, Jeddah 21589,  
Saudi Arabia

**Muhsen S. Al-Sanna**

Specialist,  
Piping and Valves Unit,  
Mechanical and Civil Engineering Division,  
Consulting Services Department,  
Saudi Aramco, Dhahran 31311,  
Saudi Arabia

# Two-Dimensional Finite Element Analysis for Large Diameter Steel Flanges

*This paper presents numerical results obtained using Finite Element Analysis (FEA) in studying large diameter welded neck steel flanges under different loading conditions. Obtained FEA results show the effect of the clamping pressure, internal pressure, axial end load, temperature effect, gasket elasticity modulus on the contact pressure between the gasket and the steel flange. As expected clamping pressure is a determinate factor for the sealing condition. Gasket material is another primary factor in designing flanged joints. [DOI: 10.1115/1.1767174]*

## 1 Introduction

Finite Element Analysis (FEA) is a powerful approximate numerical technique used to solve engineering problems. FEA has been used to model flanged joints by many researchers, see for example [1–3]. Two dimensional as well as three dimensional models have been used mainly to study the mechanics of bolted flanges. Investigated parameters include internal pressure [4], high temperature application [2], nominal pipe diameter [1], and gasket geometry [4]. Different finite element packages were used including ABAQUS [2,10] and ANSYS 5.6 [3,9].

Analyses of flange bolted joints go back to the early work of Waters et al. [5] who reformed the basis of bolted flange analyses. However, bolted flange analyses, see for example Lake and Boyd [6], including the current ASME code [7] accounts for stresses in the flange including the rim and hub stresses due to applied loads. In recent years bolted joints are designed based on tightness criteria and failure of other components, i.e., gasket collapse or bolt failure [3].

In all of the previous studies nominal pipe diameters were small and the largest reported value is 610 mm (24 in). Saudi Aramco was a pioneer in using large diameter steel flanges for steel pipelines and piping systems. In fact Saudi Aramco started using large diameter steel flanges (Nominal Pipe Size (NPS) 660 to 1424 mm [26 to 60 in]) before ASME developed their large diameter steel flanges, ASME B16.47, for NPS 26 through NPS 60 in 1990 [8].

This paper addresses stress analyses of flanged joints made up of the flange and the gasket for large diameter steel flanges. Stress analysis is directed toward the contact pressure and the gap condition between the steel flange and the gasket using two dimensional finite element analyses. Parametric studies include studying the effect of clamping pressure, internal pressure, axial end pressure, temperature and gasket material on the contact pressure.

## 2 Finite Element Modeling

The bolted joint is modeled as simplified two dimensional (two-dimensional) axisymmetric case. The line of symmetry is taken with respect to the mid-plane of the gasket while the axisymmetric line is taken with respect to the pipe axis. The two-dimensional axisymmetric quarter of the bolted joint is shown in Figs. 1 and 2. Note the gasket underneath the hub of the flange shown clearly in Fig. 2. Although the bolt hole is showing in Fig. 1, as first order

approximation, the model is taken to be away from the bolt in the middle between two successive bolts. Such approximation is common and acceptable for flange and gasket analysis purposes [3]. However, if one needs to study stresses on bolt or the contact stresses between the flange and the bolt, he has to incorporate the bolts in his two-dimensional model.

Three dimensional analysis is needed when it comes to model issues such as; the unevenness of bolt tightening, the effective gripping area of the bolt, waviness of the gasket, and other assembly problems such as lack of coaxially of the system, radial misalignment, angular misalignment and so on.

The materials used in this two-dimensional analysis are given in Table 1 for the flange and the gasket. Although the spiral ring gasket is a composite material made of asbestos fibers and a binder, it is modeled as homogenous isotropic material in the literature. Thus, the gasket is model as two dimensional isotropic homogenous entity. However, failure analysis of the gasket needs to look at it as a composite material using an appropriate anisotropic material approach. The material used for the flange is ASTM A105 steel with a 250 MPa yield strength.

Dimensions of the bolted joint are given in Table 2. The modeled flange connection is 48 inches NPS (1219 mm), 300 class with 3/4 inches (19.05 mm) shell thickness. The flange is assumed to be perfectly welded to the pipe. For assumed API 5L Grade 42 pipe the maximum permissible internal pressure is 66 bar based on yielding criteria. Figure 3 shows the finite element mesh of the joint. All solid elements assumed to be PLANE43 with four nodes and two degrees of freedom per node [9]. These elements were treated as axisymmetric elements with respect to pipe axis.

Note the very fine mesh at the gasket and the fine mesh at the stress concentration areas at the extreme ends of the rim, the rim-hub joint and the raised face fillet, as shown in Fig. 3. A contact pair is used between the gasket and the flange with the gasket as

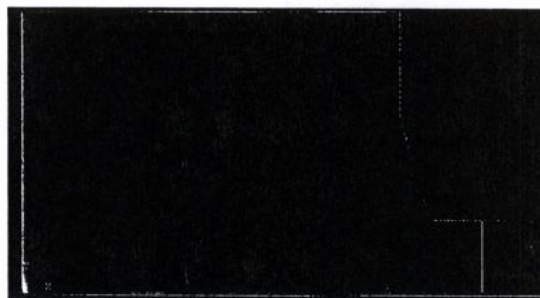


Fig. 1 The right top symmetric quarter of the flange joint

Contributed by the Pressure Vessels and Piping Division for publication in the JOURNAL OF PRESSURE VESSEL TECHNOLOGY. Manuscript received by the PVP Division August 26, 2002; revision received December 3, 2003. Associate Editor: R. Gwaltney.



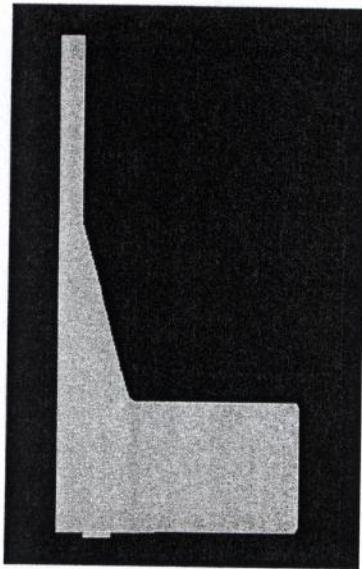


Fig. 2 The quarter axisymmetric two-dimensional model

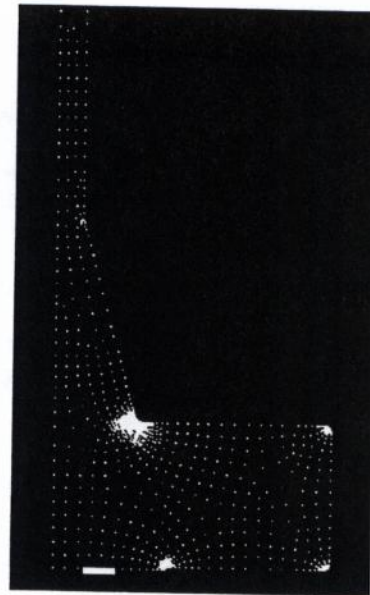


Fig. 3 The finite element mesh shown by nodes

the contact surface. Table 3 gives the loading conditions used in the parametric study. The applied boundary conditions are shown in Fig. 4.

Values given with asterisk in Table 3 are the default values. Unless otherwise stated, when changing a variable like internal pressure, other parameters are held constant to the asterisk values. The clamping pressure is varied from a minimum value of 20 MPa to a maximum value of 50 MPa, a value less than 20 MPa resulted in unstable system due to lack of the equilibrium with a 50 MPa axial pressure. Clamping pressure is assumed to be uniform throughout the effective clamping area and obtained by using 40 bolts. Clamping pressure of 20 MPa corresponds to 12.5% of the proof strength for ASTM 193 B7 bolt materials. Internal

pressures are varied from zero applied pressure to a value below yielding of the internal surfaces of the flange. The axial stress is the end hydrostatic effect due to the presence of the cover to the piping system like a blind flange. Temperature of the transported fluid sensed at the inner surface of the flange is changed from room temperature to a high value of 500°C.

The gasket modulus of elasticity is changed from low value for polymer and asbestos to high values for aluminum and steel. Vertical displacement is restricted at the lower surface of the gasket. A nonlinear FEA solution is assumed with an elastic perfectly plastic material response for the flange.

Table 1 Material properties of the joint

Part	Materials	Elastic Modulus (GPa)	Poisson's Ratio	Yield Strength (MPa)	Thermal Expansion Coefficient (m/m/°C)
Flange	Steel	200	0.3	250	15e-6
Gasket	Asbestos	5	0.33	**	**

\*\*Not Available.

Table 2 Dimensions of the joint parts

Part	Item	Unit	
Flange	Bore	mm	1143
	Bolt Circle Diameter	mm	1534
	Raised Face Diameter	mm	1372
	Flange Outer Diameter	mm	1651
	Raised Face	mm	1.588
	Smaller Outer Hub Diameter	mm	1227
	Larger Outer Hub Diameter	mm	1245
	Flange Thickness	mm	130.2
	Total Flange Length	mm	311.2
	Pipe/Shell Thickness	mm	19.05
Gasket	Gasket Outer Diameter	mm	1286
	Gasket Inner Diameter	mm	1235
	Gasket Thickness	mm	4.45
	Gasket Width	mm	25.4

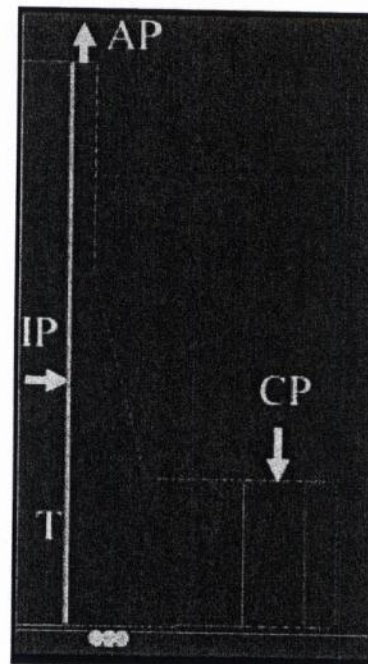


Fig. 4 Applied loadings and boundary conditions

**Table 3 The parametric study values**

Clamping Pressure, $CP$ (MPa)	Axial Pressure, $AP$ (MPa)	Internal Pressure, $IP$ (MPa)	Internal Temperature, $T$ (C°)	Gasket Modulus of Elasticity, $E_g$ (GPa)
20	0	0	25*	1
25	10	1	50	2
30*	20	2	100	5*
35	30	3*	200	10
40	40	4	300	80
50	50*	5	500	200

\*Default Values.

### 3 Results and Discussions

Obtained numerical results are shown in Figs. 5–12. Figure 5 shows the equivalent Von-Mises stress under default loading conditions, i.e., internal pressure,  $IP=3$  MPa, clamping pressure,  $CP=30$  MPa, axial pressure,  $AP=50$  MPa, temperature,  $T=25$  C° and gasket modulus of elasticity,  $E_g=5$  GPa. The minimum stress value is 2.4 MPa and the maximum one is 254 MPa which is the yield limit. Maximum values occur at the stress concentration area which is a localized value. The top side of the flange sees stress values in the range of 114 to 170 MPa; such values are acceptable for the given loading conditions. The rim of the flange undergoes less stress due to its bulkiness when compared to the tube shell, while inner areas in the rim are exposed to less stress. Looking at the gasket, one can see the gradual change in the stress from left to right. The right fibers of the gasket are exposed to more stress due to flange rotation in the clockwise

direction. This rotation caused is mainly by clamping forces and to lesser extent on the internal pressure. Stress distributions at the gasket contact surface are shown in Figs. 8–12.

A view of the Von-Mises stress contours at the gasket is shown in Fig. 6. The assumed modulus of elasticity in this image is 80 GPa corresponding to aluminum gasket. This assumption results in higher stress at the right side of the gasket but with no contact pressure on most of the gasket. Details of the contact pressure at different gasket materials will be shown later. Another image of Von-Mises stress is shown in Fig. 7 under 40 MPa clamping pressure while other defaults loads are the same. Yielding of the rim-

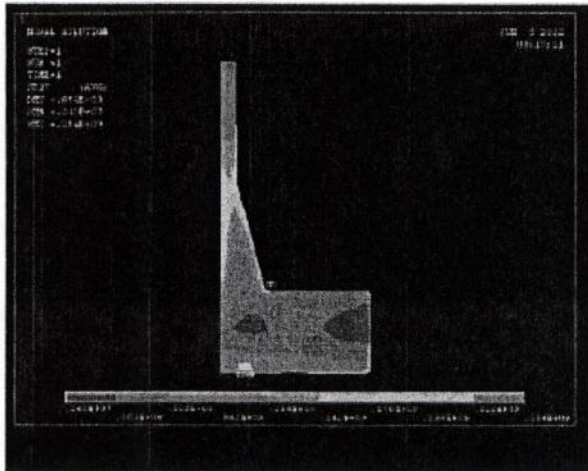


**Fig. 5** Equivalent Von-Mises stress for the flange-gasket connection under default loading conditions (see Table 3)

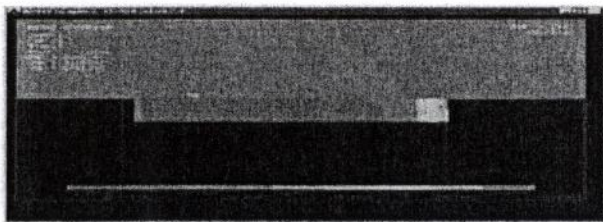


**Fig. 6** Von-Mises stress at the gasket for a gasket with a 80 GPa elastic modulus

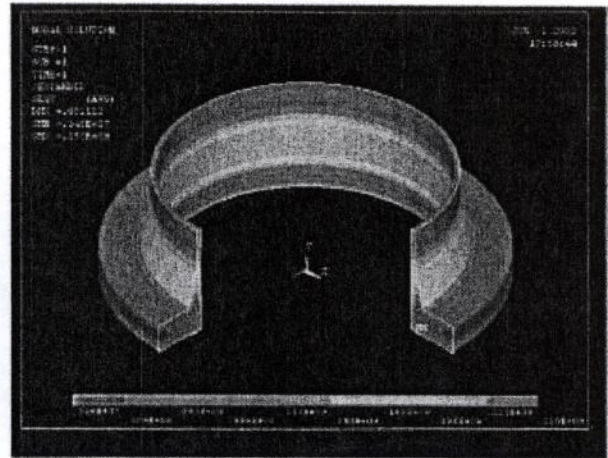


**Fig. 7** Equivalent Von-Mises stress for the flange-gasket connection under 40 MPa clamping pressure, all other loadings are the default loads

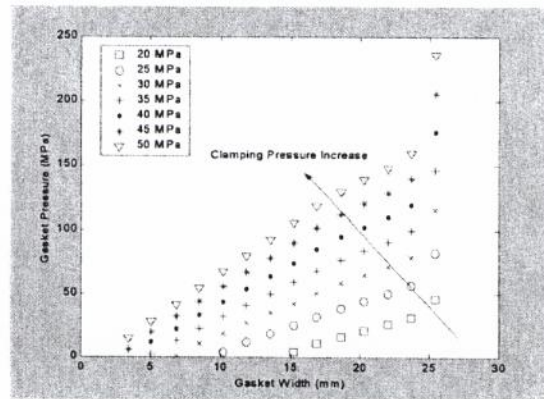


**Fig. 8** Effect of clamping pressure on gasket contact pressure



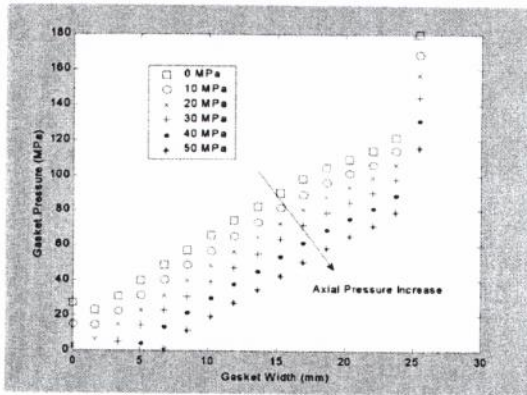


Fig. 9 Effect of axial stress on the gasket contact pressure

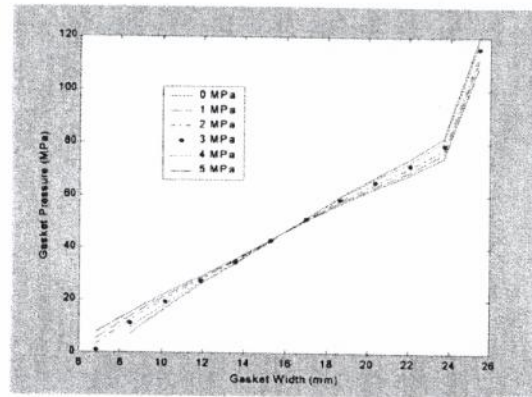


Fig. 11 Effect of internal pressure on the gasket contact pressure while neglecting end effects

hub joint area is very clear and the overall stress distribution is the same as before except the higher values due to the high clamping pressure.

**3.1 Effect of Clamping Pressure.** Clamping pressure can be varied by bolt tightening or loosening. The limiting factors for such a variable is the bolt strength and bending and bearing stresses of the flange. The direct applied clamping pressure is assumed to be uniformly distributed throughout the annular area passing through the bolt circle diameter at a width equals to bolt diameter. Due to the rigid-body rotation of the flange, the contact stress is a maximum at the right hand side of the gasket and gradually decreases from right to left. Results of the clamping pressure effect on the contact pressure are shown in Fig. 8. The vertical axis gives the contact pressure at the gasket surface in MPa while gasket width is given along the x-axis. As expected, by increasing the clamping pressure, the contact stress increases too and the gap area decreases. At a 20 MPa clamping pressure, corresponding to 12.5% of the bolt proof strength, a gap cover 60% of the gasket area and the contact pressure varies from zero to 47 MPa. By increasing the clamping pressure to 50 MPa, or 31% of the proof strength, contact pressure jumps to maximum value of 241 MPa and the gap reduces to 15% of the contact area. The nonlinear behavior of the gasket pressure at the outer diameter is attributed to the rotational effect since the last point of contact represents the center of rotation.

**3.2 Effect of Axial Stress.** Axial stress results from the presence of nearby cover to the piping system. The cover can be a

blind flange, or a *t*-section. Axial or longitudinal stress is a direct function of the internal pressure, however, axial stress is separated here, to simulate the condition of having short (with nearby blind flange) in-plant piping system from long (100s km length) pipelines. Leakage of bolted joint due to axial load or external load is a typical problem in piping engineering.

Figure 9 shows the contact pressure versus the gasket width at various axial stresses. An axial stress of 10 MPa results from an internal pressure of 627 kPa (6.2 bar) with 100% end cover efficiency. As expected, the increase in the longitudinal stress will reduce the gasket contact pressure, increase the gap at the inner diameter, start leakage and loss of the bolted joint efficiency. The partial gap caused by axial stress greater than 30 MPa is attributed to the limited applied clamping stress.

**3.3 Effect of Gasket Stiffness.** It is very well known in flanged joint design that the gasket has to be soft and durable. In Fig. 10 the gasket modulus of elasticity is changed while fixing all other variables to the default values. For the sake of easy comparison, gasket contact pressure is plotted in a log scale against linear gasket width. Gasket modulus  $E_g$  is changed from a low value of 1 GPa, corresponding to soft industrial rubber or polymer, to steel. Gap starts at  $E_g = 5$  GPa, corresponding to asbestos, and reach maximum values at  $E_g = 80$  and 200 GPa, corresponding to aluminum and steel, respectively. The increase in the contact pressure with high gasket stiffness values is obtained at a high price of losing the contact, i.e., gap expansion. The uniformity of the gasket contact pressure is obtained by softening the gasket as

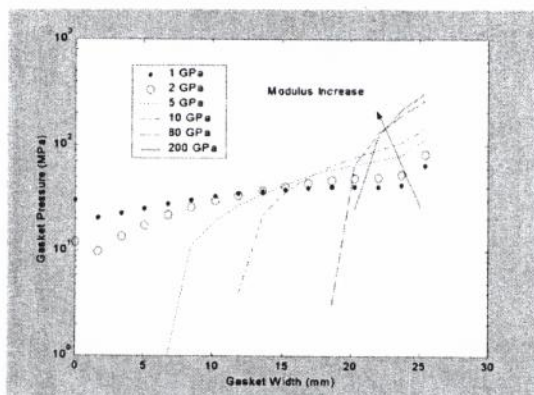


Fig. 10 Effect of gasket stiffness on the gasket contact pressure

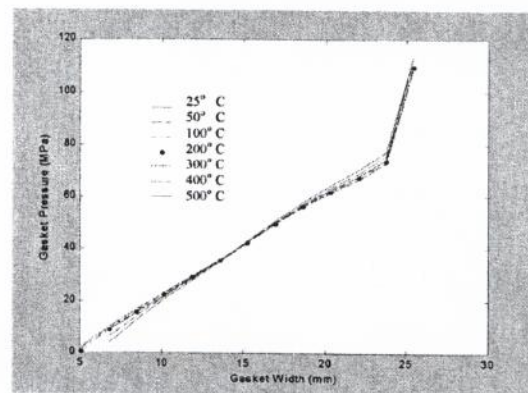


Fig. 12 Effect of fluid temperature on the gasket contact pressure

the case of  $E_g = 1$  GPa and  $E_g = 2$  GPa. Also, high stiffness gasket results in low or even zero contact pressure, see the curve corresponding to  $E_g = 5$  GPa. Linking leakage occurrence to low contact pressure is not an easy task because calculated contact pressure will be there and in a bounded value far more than the internal pressure. Leakage has to be verified with experimentation.

**3.4 Effect of Internal Pressure and Temperature.** The effect of internal pressure, at constant longitudinal stress, is shown in Fig. 11. The contact pressure between the gasket and the flange is plotted versus gasket width for different internal pressure values. One can see therefore negligible effects for the increase in the internal pressure on the contact pressure. An internal pressure increase tends to rotate the flange clockwise at slow rate (stiff rotation). Thus, for a slight increase in the contact pressure at the outer part of the gasket there is a slight reduction in the contact pressure at the inner side. Similar things can be said for the temperature effect shown in Fig. 12. An increase in temperature causes rotation of the flange due to different thermal expansion rate of the flange as the thickness changes in the vertical direction.

#### 4 Conclusions

This paper investigated the operational parameters affecting the flange-gasket assembly for large diameter steel flanges. Clamping pressure needs to be carefully selected to get proper sealing of the flange-gasket assembly. Increasing the clamping pressure will result in better contact pressure but at the cost of higher flange stresses. The gasket has to be made of a soft material with a low modulus of elasticity to ensure better sealing of the assembly. Axial end loads may result in gasket leakage since it tends to unseat the gasket if the clamping pressure is not sufficient. Internal pressure and temperature were found to be less important to the flange-gasket assembly. Experimentation to verify FEA predictions is recommended.

#### Acknowledgment

We would like to thank Saudi Aramco for their support of this study. The first author thanks King Abdulaziz University in Jed-

dah for their support during his 2001/2002 sabbatical leave. Special thanks to Salih Alidi, senior consultant engineer of the Consulting Services Department, Saudi Aramco for his valuable technical inputs to this paper. Facilitation and support provided by Mamdouh Alidarous, Fared Alhudaib and Mutaaz Mashouk is highly appreciated.

#### Nomenclature

$AP$	= axial pressure
$CP$	= clamping pressure
$E_g$	= gasket modulus of elasticity
$IP$	= internal pressure
NPS	= nominal pipe size
$T$	= temperature

#### References

- [1] Sawa, T., Higurashi, N., and Akgawa, H., 1991, "A Stress Analysis of Pipe Flange Connections," *ASME J. Pressure Vessel Technol.*, 113, pp. 497-503.
- [2] Brown, W., Derenne, M., and Bouzid, A.-H., 2001, "Determination of Gasket Stress Levels During High Temperature Flange Operation," *Analysis of Bolted Joints*, ASME PVP, 416, pp. 185-192.
- [3] Nagat, S., Shoji, Y., and Sawa, T., 2001, "The Effect of Flange Geometry Changes on the Stress Distribution Bolted Flanged Joints," *Analysis of Bolted Joints*, ASME PVP, 416, pp. 123-134.
- [4] Sawa, T., and Ogata, N., 2001, "Stress Analysis and Evaluation of the Sealing Performance in Pipe Flange Connections With Spiral Wound Gaskets Under Internal Pressure," *Analysis of Bolted Joints*, ASME PVP, 416, pp. 27-34.
- [5] Waters, E. O., Rossheim, D. B., and Williams, F. S. G., 1949, "Development of General Formulas for Bolted Flanges," *Taylor Forge and Pipe Works*.
- [6] Lake, G., and Boyd, G., 1957, "Design of Bolted Flanged Joints of Pressure Vessels," *Proc. Inst. Mech. Eng., IMechE Conf.*, 171, pp. 843-872.
- [7] ASME, 1998, ASME VIII, Div 2, Boiler and Pressure Vessel Code, ASME, NY.
- [8] ASME, 1996, ASME B16.47, Large Diameter Steel Flanges, NPS 26 Through NPS 60, ASME, NY.
- [9] ANSYS 5.6 Manual, 2002, ANSYS Inc., Canonsburg, PA.
- [10] ABAQUS 6.1 Standard Manual, 2002, HKS Inc., Pawtucket, RI.